Linking in Systems with One-dimensional Periodic Boundaries

Kenneth Millett *
Eleni Panagiotou †

August 25, 2016

Abstract

With a focus on one-dimensional periodic boundary systems, we describe the application of extensions of the Gauss linking number of closed rings to open chains and, then, to systems of such chains via the periodic linking and periodic self-linking of chains. These lead to the periodic linking matrix and its associated eigenvalues providing measures of entanglement that can be applied to complex systems. We describe the general one-dimensional case and applications to one-dimensional Olympic gels and to tubular filamental structures.

1 Introduction

The objective of this report is to describe the application of the Gauss linking number [7] to collections of open chains in models of filamental systems that employ periodic boundary conditions (PBC). These enable one to define periodic linking and periodic self-linking numbers [15, 16] that quantify the linking between pairs of filaments and, thereby, define the periodic linking matrix. The information they provide has been studied in several one-dimensional PBC models, fore example: general systems such as polymer gels [13], Olympic gels [9], and filamental structures in a long tube [12], see Figure 1.

In the next section we describe the Gauss linking and self-linking numbers, one-dimensional periodic boundary condition models, the extension to periodic linking and self linking, and the definition of the periodic linking matrix whose eigenvalues quantify the extent of entanglement in the systems to which they are applied. We will then describe instances in which the periodic linking matrix provides important information in the study of general systems such as polymer gels, Olympic gels, and filamental structures such as vortex flow lines in tubes.

*Department of Mathematics,University of California, Santa Barbara, CA 93106, USA
†Department of Mathematics,University of California, Santa Barbara, CA 93106, USA

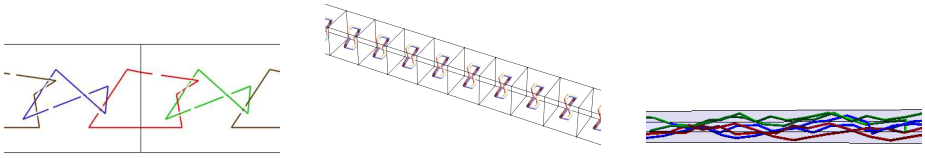

Figure 1: A general 1PBC example, an Olympic system, and filamental structure in a tube.

2 Gauss Linking, Periodic Boundary Condition (PBC) Models, Periodic Linking, and the Periodic Linking Matrix

2.1 Gauss Linking and Self-linking

The linking number between two oriented chains, l_1 and l_2, is defined using parameterizations of the chains, $\gamma_1(t)$ *and* $\gamma_2(s)$, via the Gauss linking integral:

Definition 2.1. The Gauss *linking number* of two disjoint (closed or open) oriented curves l_1 and l_2, whose arc-length parametrizations are $\gamma_1(t), \gamma_2(s)$ respectively, is defined as a double integral over l_1 and l_2 [7]:

$$L(l_1, l_2) = \frac{1}{4\pi} \int_{[0,1]} \int_{[0,1]} \frac{(\dot{\gamma}_1(t), \dot{\gamma}_2(s), \gamma_1(t) - \gamma_2(s))}{||\gamma_1(t) - \gamma_2(s)||^3} dtds, \tag{1}$$

where $(\dot{\gamma}_1(t), \dot{\gamma}_2(s), \gamma_1(t) - \gamma_2(s))$ is the triple product of $\dot{\gamma}_1(t), \dot{\gamma}_2(s)$ and $\gamma_1(t) - \gamma_2(s)$.

Definition 2.2 (Self-linking number)**.** Let l denote a chain, paramerterized by $\gamma(t)$, then the *self-linking number* of l is defined as:

$$\begin{aligned} Sl\,(l) \quad &= \tfrac{1}{4\pi} \textstyle\int_{[0,1]^*} \int_{[0,1]^*} \frac{(\dot{\gamma}(t), \dot{\gamma}(s), \gamma(t) - \gamma(s))}{||\gamma(t) - \gamma(s)||^3} dtds \\ &\quad + \tfrac{1}{2\pi} \textstyle\int_{[0,1]} \frac{(\gamma'(t) \times \gamma''(t)) \cdot \gamma'''(t)}{||\gamma'(t) \times \gamma''(t)||^2} dt. \end{aligned} \tag{2}$$

The self-linking number consists of two terms, the first being the Gauss integral and the second being the total torsion of the curve.

2.2 One-dimensional Periodic Boundary Condition Models

The underlying structure of the *Periodic Boundary Condition*, PBC, model employed in this study consists of a cube or a solid right cylinder whose x length is one and whose y and z coordinates lie within the unit square or, respectively, in a disc of radius $a > 0$. The three-dimensional body contains a collection of

arcs whose endpoints either lie in the interior or intersect the $x = 0$ or $x = 1$ faces under the constraint that the pattern on both faces is identical, see Figure 1. The later condition allows one to create and infinite structure by taking the union of integer translates of the cells and taking the unions of the resulting one-chains to define a collection of one dimensional chains. As, in general, these chains may be non-compact, we will require that each chain has precisely the same number of edges, N, thereby imposing one aspect of homogeneity. Due to the PBC structure, there is also a large scale homogeneity in the collection of chains.

2.3 Periodic Linking and Self-linking

In a PBC model, each chain is translated to give an infinite collection copies of itself. As a consequence, one is faced with quantifying the linking of one chain, l_0 with infinitely many translation copies of itself, $l_v = l_0 + \vec{v}$, or with infinitely many copies of another chain, $J_v = J_0 + \vec{v}$. This is achieved by employing Panagioutou's periodic linking and self-linkings numbers described next. In the periodic system we define linking at the level of free chains (i.e. the collection of translation copies of a chain, l_0; see [15] for a discussion of the motivation for this definition). The underlying idea is to calculate the linking between the generating chain in one with all the chains in the other free chain.

Definition 2.3 (Periodic linking number)**.** Let I and J denote two (closed, open or infinite) free chains in a periodic system. Suppose that I_0 is an image of the free chain I in the periodic system. The *periodic linking number*, LK_P, between two free chains I and J is defined as:

$$LK_P(I, J) = \sum_{\vec{v} \neq \vec{0}} L(I_0, J_0 + \vec{v}), \tag{3}$$

where the sum is taken over all the images of the free chain J in the periodic system.

The periodic linking number has the following properties with respect to the structure of the cell, see [15], which follow directly by its definition:
(i) The infinite sum defining LK_P converges, i.e. LK_P makes sense mathematically.
(i) LK_P captures all the linking that all the images of a free chain impose to an image of the other.
(ii) LK_P is independent of the choice of the image I_0 of the free chain I in the periodic system.
(iii) LK_P is independent of the choice, the size and the shape of the generating cell.
(iv) LK_P is symmetric.

The quantification of the linking of a free chain with itself is a bit special and requires a bit more care as there are two contributing cases, the linking of

a chain with itself and the linking of a chain with translations of itself. As a consequence, one is lead to the following definitions [15]:

Definition 2.4 (Periodic self-linking number)**.** Let I denote a free chain in a periodic system and let I_0 be an image of I, then the *periodic self-linking number* of I is defined as:

$$SL_P(I) = Sl(I_0) + \sum_{v \neq u} L(I_0, I_v), \tag{4}$$

where the index v runs over all the images of I, except I_0, in the periodic system.

As with the periodic linking number, the mathematical proof of its existence of this quantity and its properties are proved in [15].

2.4 Periodic Linking Matrix

In order to analyze the linking entanglement present in our PBC system, L, consisting of a finite number of free chains, $l_1, l_2, ..., l_n$, we employ an n x n real symmetric matrix, M(L), whose i, jth entry is defined by equation

$$\begin{aligned} M(L)_{i,i} &= SL_P(l_i) \\ M(L)_{i,j} &= LM_C(l_i, l_j) \end{aligned} \tag{5}$$

In the case of a single generating chain, l, the periodic linking matrix consists of a single entry, the periodic self-linkng number, $Sl(l)$. From the definitiion, there are two contributing factors, the self-linking given by the equation 2 and the linking between distinct copies, reflecting distinct features of periodic self-linking.

For systems with two independent chain types, the periodic linking matrix adds entanglement information due to the linking between the two distinct chains. Associated to the periodic linking matrix are two real eigenvalues, $e_1(L)$ and $e_2(L)$, given in decreasing order. The larger of these, $e_1(L)$ is proposed as the dominant characterization of the linking entanglement of the PBC system. The set of eigenvalues is the *periodic linking spectrum* of the system.

Similarly, for systems with n independent chain types, one defines the periodic linking matrix, M(L),. The associated ordered collection of eigenvalues, $e_1(L), ..., e_n(L)$ define the spectrum of the PBC system.

3 General Systems, Olympic Systems, Tubular Systems

3.1 General Systems

For computational efficiency, only a small portion of the physical system is simulated and periodic boundary constraints are used to avoid boundary effects.

The size of the simulation cell may influence the results of a computational experiment. We examine how the periodic linking matrix changes with respect to the size of the simulation cell.

By concatenating m cells we obtain a larger cell that we denote mC, which applies PBC to the chains that touch its faces in the $x-$direction. We can concatenate cells of the type mC by gluing their $x-$faces with respect to the PBC, in order to create the same periodic system that is generated by the cell C. In this section we study the periodic linking matrix of a periodic system as the size of the cell used for its simulation, characterized by m, increases. We will see that the linking matrix depends on the size of the cell used for the simulation of a system. Since the periodic system simulated is the same, one would expect the periodic linking matrix to retain certain entanglement information. However, we will see that in a topological sense, these systems are different. With our study we extract entanglement information that is invariant of the cell size as well as information that depends on it.

Let C denote a cell composed by n generating chains, and let LM_C denote the corresponding periodic linking matrix of size $n\times n$. Without loss of generality we will concatenate cells always to the positive direction of the $x-$axis. Let mC denote the cell that results by gluing m copies of C respecting the PBC. Then mC has more chains. More precisely:

Lemma 3.1. *Let C be a cell with n generating chains. Then the cell mC that results by gluing m copies of C respecting the PBC, has mn generating chains.*

Remark 3.2. The different generating chains in mC generate different free chains in the periodic system. We denote the free chains in mC generated by $i^{(j)}$, $j = 0, \ldots, m-1$, as $I^{(j)} = I^{(0)} + \vec{v}_j$.

Thus the corresponding periodic linking matrix, LM_{mC} has size $mn \times mn$. Indeed, the cells C and mC describe different topological objects. If we identify the faces of the cell, then we will get an $n-$component link in the solid torus in the first case and a $mn-$component link in the second case. The 3-manifolds are the same in both cases even though the links that they contain are different, related by an $m-$fold covering space of the second manifold over the first. So, we notice that the linking matrices LM_C and LM_{mC} are different, but the periodic system that the cells generate and whose entanglement we wish to measure, is the same. For this purpose, we will study the dependence of the periodic linking matrix on the cell size and we will look for quantities that remain invariant of cell size.

In the following we will prove that some of the eigenvalues of the periodic linking matrix are independent of cell size. First we will study the simplest case of the periodic linking matrix of a single chain in a cell with one PBC. Next, we will generalize this to the case of n chains in a cell with one PBC. This case will facilitate the understanding of the general case of systems employing one PBC. The methods presented here can also be used to obtain similar results in 2 and 3 PBC.

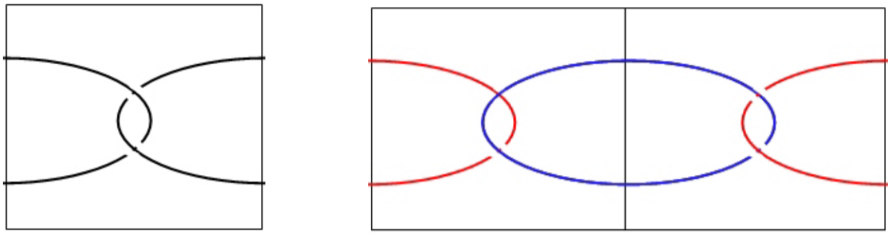

Figure 2: One chain in a system with one PBC. Left: The original cell C contains 1 generating chain. Right: The cell $2C$ contains 2 generating chains.

We will next study the case of a cell with one PBC that contains one generating chain that unfolds in k cells. The periodic linking matrix of that system has size 1×1, $LM_C = SL_P(I) = Sl(I_0) + \sum_i L(I_0, I_i)$.

If we concatenate m cells to create a larger cell mC, then by Lemma 3.1 there are m generating chains in k_1C, we denote $I^{(0)}, I^{(1)} = I^{(0)} + (1,0,0), \ldots, I^{(m)} = I^{(0)} + (m,0,0)$ (see Figure 2). The linking matrix for this cell has size $m \times m$ and has the following form:

$$LM_{mC} = \begin{bmatrix} SL_P(I^{(0)}) & LK_P(I^{(0)}, I^{(1)}) & \ldots & LK_P(I^{(0)}, I^{(m-1)}) \\ LK_P(I^{(0)}, I^{(1)}) & SL_P(I^{(1)}) & \ldots & LK_P(I^{(1)}, I^{(m-1)}) \\ \ldots & \ldots & \ldots & \ldots \\ LK_P(I^{(0)}, I^{(m-1)}) & LK_P(I^{(1)}, I^{(m-1)}) & \ldots & SL_P(I^{(m-1)}) \end{bmatrix} \tag{6}$$

Lemma 3.3. *Let C denote a cell with one PBC that consists of only one chain, I. Let mC denote the cell that results after gluing m copies of C, then LM_{mC} is a symmetric centrosymmetric matrix.*

Proposition 3.4. *Let I denote a chain in a cell C with one PBC. Let mC denote the cell that results after gluing m copies of C. Then the j-th eigenvalue of LM_{mC} is given by:*

$$\lambda_j = SL_P(I^{(0)}) + 2\sum_{k=1}^{\frac{m-1}{2}} LK_P(I^{(0)}, I^{(k)}) \cos\Big(\frac{2\pi}{m} k(j-1)\Big) \tag{7}$$

for m odd and

$$\begin{aligned} \lambda_j =& SL_P(I^{(0)}) + (-1)^{(j-1)} LK_P(I^{(0)}, I^{(\lfloor \frac{m-1}{2} \rfloor + 1)}) \\ &+ 2\sum_{k=1}^{\lfloor \frac{m-1}{2} \rfloor} LK_P(I^{(0)}, I^{(k)}) \cos\Big(\frac{2\pi}{m} k(j-1)\Big) \end{aligned} \tag{8}$$

for m even.

Remark 3.5. . (i) λ_1 is independent of cell-size, m and $\lambda_1 = SL_P(I)$ for all m.

(ii) There are at most $1 + \lfloor \frac{m-1}{2} \rfloor$ distinct eigenvalues, as expected for real circulant matrices [17]. Indeed, notice that $\sin^2\Big(\frac{2\pi(j-1)}{m}\Big) = \sin^2\Big(\frac{2\pi(m-(j-1))}{m}\Big)$ and $\cos\Big(\frac{2\pi(j-1)}{m}\Big) = \cos\Big(\frac{2\pi(m-(j-1))}{m}\Big)$. Therefore, $\lambda_j = \lambda_{m-j+2}$ for all $j > 1$.

(iii) For closed chains and for $m > 2|mu(I_0)|$, the j-th eigenvalue of the linking matrix has a simpler formula, namely:

$$\lambda_j = Sl(I_0) + 2\sum_{k=1}^{\frac{m-1}{2}} L(I_0, I_0 + (k,0,0)) \cos\Big(\frac{2\pi}{m} k(j-1)\Big) \tag{9}$$

for m odd and

$$\begin{aligned} \lambda_j &= Sl(I_0) + (-1)^{(j-1)} L(I_0, I_0 + ((\lfloor \frac{m-1}{2} \rfloor + 1), 0, 0) \\ &+ 2\sum_{k=1}^{\lfloor \frac{m-1}{2} \rfloor} L(I_0, I_0 + (k,0,0)) \cos\Big(\frac{2\pi}{m} k(j-1)\Big) \end{aligned} \tag{10}$$

for m even.

Remark 3.6. The difference between the first two eigenvalues of LM_{mC} is:

$$\begin{aligned} \lambda_1 - \lambda_2 &= SL_P(I^{(0)}) + 2\sum_{k=1}^{\frac{m-1}{2}} LK_P(I^{(0)}, I^{(k)}) - SL_P(I^{(0)}) \\ &- 2\sum_{k=1}^{\frac{m-1}{2}} LK_P(I^{(0)}, I^{(k)}) \cos\Big(\frac{2\pi}{m} k\Big) \\ &= 2\sum_{k=1}^{\frac{m-1}{2}} LK_P(I^{(0)}, I^{(k)})(1 - \cos\Big(\frac{2\pi}{m} k\Big)) \end{aligned} \tag{11}$$

for m odd and

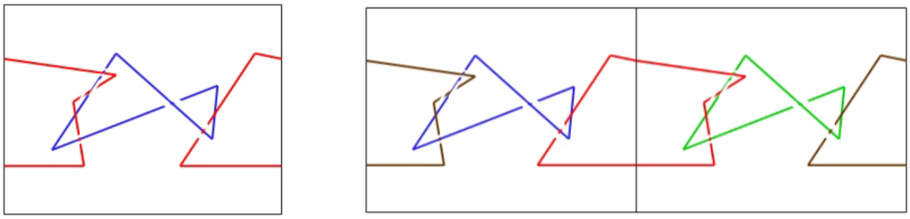

Figure 3: 2 chains in a system with one PBC. Left: The original cell C contains 2 generating chains. Right: The cell $2C$ contains 4 generating chains.

$$\begin{aligned}\lambda_1 - \lambda_2 &= SL_P(I^{(0)}) + LK_P(I^{(0)}, I^{(\lfloor \frac{m-1}{2} \rfloor + 1)}) + 2 \sum_{k=1}^{\lfloor \frac{m-1}{2} \rfloor} LK_P(I^{(0)}, I^{(k)}) - SL_P(I^{(0)}) \\ &- LK_P(I^{(0)}, I^{(\lfloor \frac{m-1}{2} \rfloor + 1)}) - 2 \sum_{k=1}^{\lfloor \frac{m-1}{2} \rfloor} LK_P(I^{(0)}, I^{(k)}) \cos\Big(\frac{2\pi}{m} k\Big) \\ &= 2 \sum_{k=1}^{\lfloor \frac{m-1}{2} \rfloor} LK_P(I^{(0)}, I^{(k)})(1 - \cos\Big(\frac{2\pi}{m} k\Big)) \end{aligned} \tag{12}$$

for m even.

The above formula shows that the difference between the first eigenvalues does not depend on the self-linking number of the chain. The formula indicates that the difference, which is a measure of the homogeneity of the entanglement, is a weighted function of the linking numbers of the chain with its images. Interestinlgy, for large m, the linking with the nearest images contributes less than the linking with further images.

Remark 3.7. Often in applications one is interested in the average properties of filaments. Cancellations may occur when using the Gauss and periodic linking number. For this reason, one may want to use the absolute values of all the entries of the periodic linking matrix, we call the *absolute periodic linking matrix*. The absolute periodic linking matrix is also symmetric centrosymmetric. Lower bounds on the maximum eigenvalue of nonnegative real symmetric centrosymmetric matrices can be found in [17].

Next, we will extend our previous results to the case of n chains in a system with one PBC.

Let us consider n chains, say $H1, H2, \ldots, Hn$ in a system with one PBC that unfold in $k_i, i = 1, \ldots, n$ cells each. The periodic linking matrix of that system has size $n \times n$,

$$LM_C = \begin{bmatrix} SL_P(H1) & LK_P(H1,H2) & \dots & LK_P(H1,Hn) \\ LK_P(H1,H2) & SL_P(H2) & \dots & LK_P(H2,Hn) \\ \dots & & & \\ LK_P(H1,Hn) & LK_P(H2,Hn) & \dots & SL_P(Hn) \end{bmatrix} \tag{13}$$

Then the matrix LM_{mC} has size $mn \times mn$, since to each free chain, Hj, of the cell C, correspond m free chains, $Hj^{(i)}$, $i = 0, \dots, m-1$, in the cell mC (see Lemma 3.1) (see Figure 3). We make the convention that the u-th row of LM_{mC}, where $u = rm + l$ corresponds to the free chain $H(r+1)^{(l-1)}$. Therefore, the (q, w)-th element of LM_{mC}, where $q = q_1 m + q_2, w = w_1 m + w_2$, is: $LK_P(H(q_1+1)^{(q_2-1)}, H(w_1+1)^{(w_2-1)})$.

Proposition 3.8. *Let C denote a cell with one PBC that consists of n chains. Let mC denote the cell that results after gluing m copies of C, then LM_{mC} can be expressed as an $n \times n$ block matrix of $m \times m$ symmetric circulant matrices. Moreover, the diagonal block matrices are symmetric centrosymmetric matrices. The eigenvalues of the (i,i)-th block of LM_{mC}, $i = 1, \dots, n$, are:*

$$\lambda_s = SL_P(Hi^{(0)}) + 2\sum_{k=1}^{\frac{m-1}{2}} LK_P(Hi^{(0)}, Hi^{(k)}) \cos\Big(\frac{2\pi}{m} k(s-1)\Big) \tag{14}$$

for m odd and

$$\begin{aligned} \lambda_s = {} & SL_P(Hi^{(0)}) + (-1)^{(s-1)} LK_P(Hi^{(0)}, Hi^{(\lfloor \frac{m-1}{2} \rfloor + 1)}) \\ & + 2\sum_{k=1}^{\lfloor \frac{m-1}{2} \rfloor} LK_P(Hi^{(0)}, Hi^{(k)}) \cos\Big(\frac{2\pi}{m} k(s-1)\Big) \end{aligned} \tag{15}$$

for m even, $s = 1, \dots, m$.

The eigenvalues of the (i,j)-th block of LM_{mC}, $1 \le i < j \le n$, are:

$$\lambda_s = LK_P(Hi^{(0)}, Hj^{(0)}) + 2\sum_{k=1}^{\frac{m-1}{2}} LK_P(Hi^{(0)}, Hj^{(k)}) \cos\Big(\frac{2\pi}{m} k(s-1)\Big), \tag{16}$$

for m odd and

$$\begin{aligned} \lambda_s = {} & LK_P(Hi^{(0)}, Hj^{(0)}) + (-1)^{(s-1)} LK_P(Hi^{(0)}, Hj^{(\lfloor \frac{m-1}{2} \rfloor + 1)}) \\ & + 2\sum_{k=1}^{\lfloor \frac{m-1}{2} \rfloor} LK_P(Hi^{(0)}, Hj^{(k)}) \cos\Big(\frac{2\pi}{m} k(s-1)\Big) \end{aligned} \tag{17}$$

for m even, $s = 1, \dots, m$.

Notice that in the case of n chains in a system with 1 PBC the periodic linking matrix is no longer a circulant matrix and its eigenvalues are not known. However, the eigenvalues of its block matrices are known. More precisely, LM_{mC} can be expressed as

$$LM_{mC} = \Sigma M + \Lambda M \tag{18}$$

where $\Sigma M, \Lambda M$ are $m \times m$ block matrices. ΣM is a diagonal block matrix, whose blocks represent the linking of a chain Hi with its own images and are symmetric centrosymmetric. ΛM is a block matrix whose diagonal matrices are zero and its off-diagonal matrices represent the linking between different generating chains, and are symmetric circulant matrices

The following Proposition shows that some of the eigenvalues of the periodic linking matrix are invariant of cell-size, m.

Proposition 3.9. *Let LM_C be the periodic linking matrix of a periodic system generated by the cell C with one PBC, which contains n chains. Then any other periodic linking matrix LM_{mC} of the same periodic system generated by the cell mC is of the form*

$$LM_{mC} = \begin{bmatrix} LM_C & E \\ 0 & F \end{bmatrix} \tag{19}$$

where E has size $1 \times (m-1)$ and F has size $(m-1) \times (m-1)$.

Remark 3.10. From Proposition 3.9 it follows that the eigenvalues of LM_C are among the eigenvalues of LM_{mC}, for all m.

3.2 Olympic Systems

Olympic systems are collections of small ring polymers whose aggregate properties are largely characterized by the extent (or absence) of topological linking in contrast with the topological entanglement arising from physical movement constraints associated with excluded volume contacts or arising from chemical bonds. These were first discussed by de Gennes [3] and have been of interest ever since due to their particular properties and their occurrence in natural organisms, for example as intermediates in the replication of circular DNA in the mitochondria of malignant cells or in the kinetoplast DNA networks of trypanosomes [2, 10, 11, 4, 5, 1, 6]. In this project, we studied systems that have an intrinsic one, two, or three dimensional character and consist of large collections of ring polymers modeled using periodic boundary conditions. In this report we will focus on the one-dimensional facets of these structures, see Figure 4. We identified and discussed the evolution of the dimensional character of the large scale topological linking as a function of density. We identified the critical densities at which infinite linked subsystems arise, the onset of percolation, in the periodic boundary condition systems. We showed that, with increasing density, the topological entanglement of these systems increases in complexity, dimension, and probability.

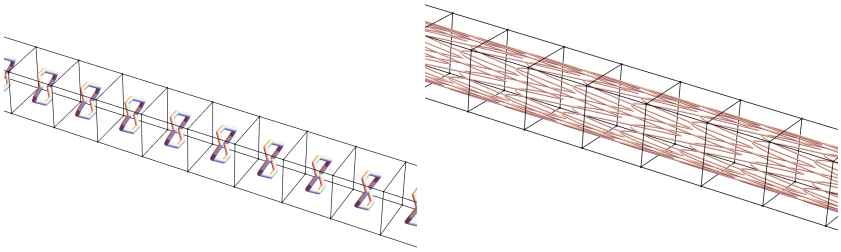

Figure 4: 1D PBC Systems: Unlinked and Saturated

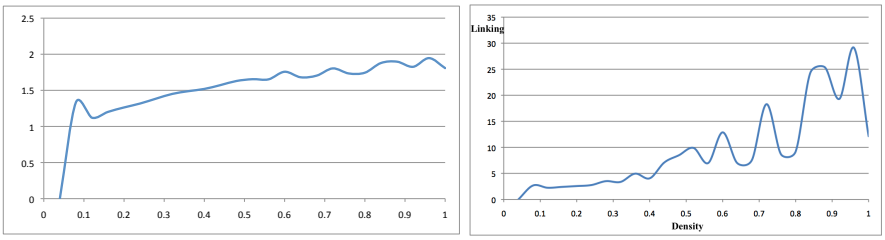

Figure 5: The mean absolute linking of two chains and the mean total absolute linking per chain as a function of density for 1PBC saturated systems.

3.2.1 Analysis of One-Dimensional PBC Olympic Systems

The mean absolute linking number in saturated systems in 1 PBC becomes greater than zero at density $\rho \approx 0.08$, when the mean valence and the probability of percolation become non-zero, see Figure 5. It is interesting to notice that the mean absolute linking number exceeds one, showing that, even though the polygons are not knotted and are just close enough to link, there exist polygons with absolute linking greater than one. At the critical density the mean absolute linking becomes 1.3, indicating the presence of many pairs of polygons with absolute linking number greater than one. The mean absolute linking number continues to increase with density, approaching the value 2. This suggests that at high densities unknotted polygons can have high linking numbers, a conclusion supported by the growth of the total absolute linking as a function of the density.

3.2.2 Percolation Analysis

For PBC Olympic systems, we proposed the following relationship between the probability of total saturation as a function of the density of the system:

$$p(\rho) = \frac{1}{1 + \rho^{-\alpha} e^{-k\rho}}$$

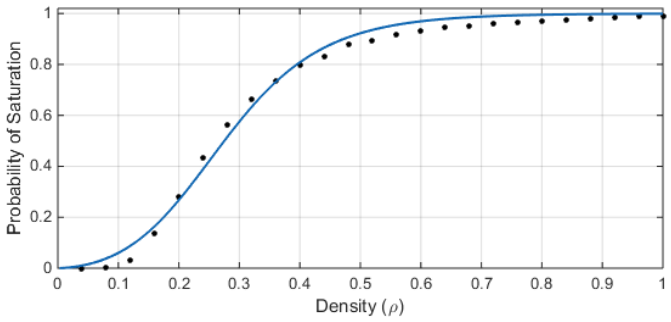

Figure 6: The observed probability of saturation in a one dimensional PBC System as a function of density plotted against its fitting curve $p(\rho)$

as inspired by the logistic equation where ρ is the density, $\alpha = n + \frac{1}{2}$, n is the dimension of the PBC system, and k is a constant.

Note that a polygon can link with one of its translations when the size of the simulation box is similar to the size of the chain. On average, a polygon will link with its own image when the length of the simulation cell is $l \approx 2\langle R_g^2 \rangle^{1/2} \approx 2 \cdot 3.23 = 9.12$, which corresponds to a density of $\rho = \frac{1}{6.45} = 0.15$ for rings. More precisely, in a system with one, two, or three PBC, when the length of the cell is $l < 2\lambda_n$.This implies that we should expect linking to occur when $l \leq 2\lambda_1$ givine a critical density of $\rho_{C1} > \frac{1}{11.94} = 0.0837521$ for a one-dimensional system.

In a one dimensional PBC system, see Figure 6, we notice that the probability of saturation becomes greater than 0 at $\rho \approx 0.12$, in agreement with our analysis. In a one dimensional PBC system, more than half of the conformations are fully saturated once the density has exceeded 0.28. Using *Matlab*'s non-linear fitting, we find $k = 7.032$ with an $R^2 = 0.9918$, see Figure 6. This suggests that the probability of linking between two translations of a polygon as a function of density is:

$$p(\rho) = \frac{1}{1 + \rho^{-1.5} e^{-7.032\rho}}$$

to be compared with the probability of linking between two random unknotted polygons provided in [8].

3.2.3 Analysis of Valence, $|V|$

In this section we discuss the mean valence, $|V|$, of a polygon in a percolated system, i.e. the average number of polygons with which an individual polygon may link. Recalling that the typical enveloping ellipsoid has characteristic radii of $\lambda_1 = 5.97, \lambda_2 = 4.09$, and $\lambda_3 = 2.9$ [14], let us denote by I_0 a random polygon of N unit length edges in a system with n =1, 2, or 3 PBC and defined by its generating cell of dimensions l_x, l_y, l_z. We propose that I_0 may link any

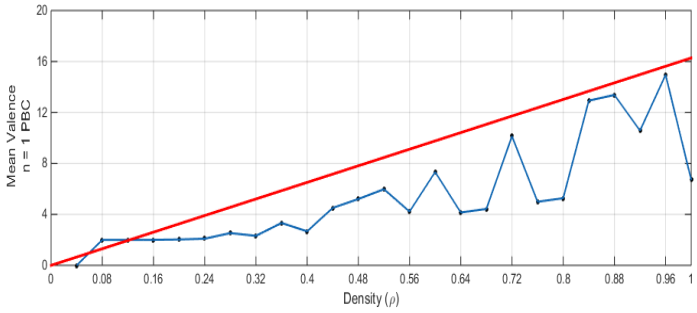

Figure 7: Mean valence of the total 1PBC system superimposed with the analytical model. We notice that $< |V| >_{1PBC} \leq 16.28\rho$, as expected.

of its own translations if the enveloping ellipsoid of the translation intersects the enveloping ellipsoid of I_0. To obtain an estimate of the valence, we first consider the enveloping ellipsoid of I_0 and form a shell around it by adding a thickness proportional to the characteristic radii in the nearest direction ie. $\lambda_n \frac{<Rg^2>^{1/2}}{\lambda_1}$. The respective radii defining this shell are then $(\lambda_1 + \lambda_1 \frac{<Rg^2>^{1/2}}{\lambda_1})$, $(\lambda_2 + \lambda_2 \frac{<Rg^2>^{1/2}}{\lambda_1})$, $(\lambda_3 + \lambda_3 \frac{<Rg^2>^{1/2}}{\lambda_1})$. We estimate the valence by counting the number of images whose center of gravity are contained within this volume by dividing by the volume of the generating cell. Setting the static dimensions of the generating cell equal to $2 * \lambda_n$, we find the following estimates for mean valence in an n-PBC system:

$$< |V| >_{n-PBC} \quad \leq \quad \frac{\frac{4}{3}\pi\lambda_1\lambda_2\lambda_3(1 + \frac{<Rg^2>^{1/2}}{\lambda_1})\rho^n}{(2\lambda_{n+1})^{(3-n)}}$$

.

Using the appropriate values of n, we bound the mean valence in each system of PBC's by:

$$\begin{aligned} < |V| >_{1PBC} \quad &\leq \quad 16.28\rho \\ < |V| >_{2PBC} \quad &\leq \quad 296.61\rho^2 \\ < |V| >_{3PBC} \quad &\leq \quad 1089.03\rho^3 \end{aligned}$$

We expect these to be upper bound estimates, especially at higher densities, due to the over counting of some portion of cells whose centers are not within the shell. However, the combined volume of those on the boundary of the shell could add to this count.

The mean valence of a saturated system in 1 PBC becomes non-zero at 2 for $\rho \geq 0.12$ corresponding with the critical density for filamental percolation $\rho_{C1} > 0.0836$. The mean valence continues to increase non-monotonically thereafter, see Figure 7. Notice that, at the saturation density of $\rho = 0.28$, we have a mean valence of approximately 2.53, indicating that at least a fourth of the linked polygons link with their second order neighbors. This saturation density

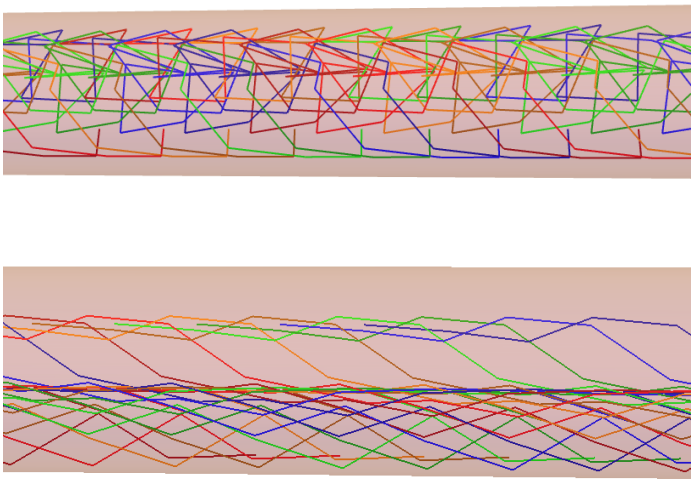

Figure 8: PBC Examples: unit radius disc cross-section, single chain of length 25. Left, 0.00 alignment constraint (random) and, second, 0.50 alignment constraint.

corresponds to an edge length of $l \approx 3.57 < 2\lambda_1$, which explains why the mean valence becomes greater than two.

3.3 Vortex Flow in Tubular Systems

In Figure 8 we show a simple example of a length 25 chains contained in a tube whose cross-sectional disc of radius 1 under an alignment constraint scaled to 0.00 and 0.50. We interpret these chains as representing short vortex flow lines in a tubular system and will focus on the case in which there are three independent PBC families of chains generating the structure representing the flow lines, see Figure 8.

For these filamental structures, we systematically studied a range of lengths, tube cross-sections, and scaled alignment conditions in order to estimate how these fundamental parameters influenced the shape and entanglement that depend upon them. For example, for a sample size of 500, the random chains in the unit radius tube have an average tube length of 7.86 units with an average radius of gyration of 3.57, see Figure 9. The average absolute self-linking is 1.09, see Figure 10. As a measure of entanglement, we find the average maximal, medial, minimal absolute eigenvalues of the linking matrix to be 1.18,

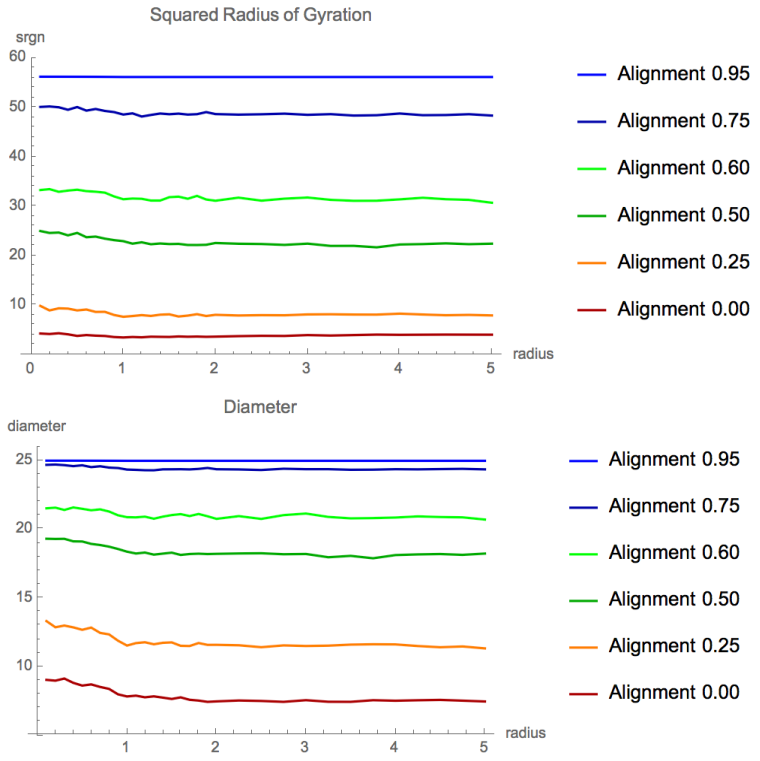

Figure 9: The mean squared radius of gyration and diameter of 25 step chains as a function of the tube radius and alignment constraint

1.01 and, 0.46 respectively. In contrast, for an alignment condition of 0.50, one has an average tube length of $18,35$ with a radius of gyration of 22.77 and an average absolute self-linking of 1.34. The absolute eigenvalues have averages of 2.20, 1.27, and 0.57 respectively. The increased level of entanglement found in aligned systems compared to a fully random system is a key result of our analysis of the filamental structure's dependence upon cross-sectional constraints and alignment.

In Figure 11 we show the evolution of the absolute values of the three eigenvalues of a PBC system generated by three independent filaments of length 25. Here, one observes a decreasing tendency in the magnitude of the eigenvalues with increasing tube radius and an increasing tendency with increasing alignment constraint. While one may expect a random system to exhibit a stronger degree of entanglement, we have seen that these filaments have smaller diameter (or squared radius of gyration) thereby offering them a significantly smaller

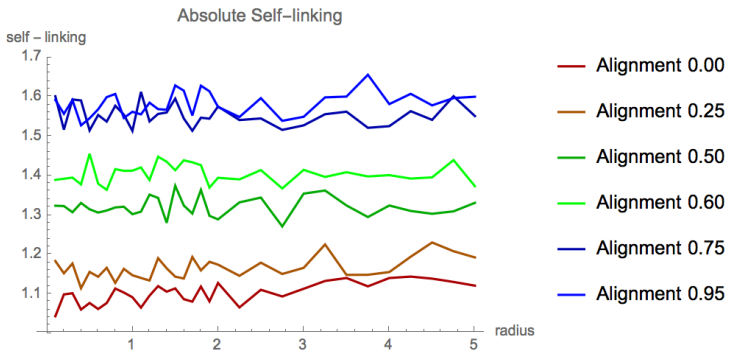

Figure 10: Absolute self-linking of single 25 step chains as a function of alignment constraint and tubular radius

opportunity to entangle with nearby filaments whereas filaments subject to an alignment constraint have a significantly larger number of adjacent filaments with which they may entangle. Thus, we see that the magnitude of the eigenvalues increase with increasing alignment. In addition, for a fixed alignment constraint, the magnitude of the eigenvalues decreases with increasing tube radius across the range of radii presented here, i.e. from 0.1 through 5.0 showing that the filamental structure widely explores the cylindrical tube leading to a decreasing density leading to decreasing entanglement.

Consistent with our earlier analysis, we find that a random system displays the smallest entanglement as measured by the magnitude of the eigenvalues, see Figure 12. In Figure 13 we see that the two eigenvalues of larger magnitudes are rather larger than the random system but tend to get smaller with increasing tube radius while the smallest is relatively stable in magnitude. Since the character of this decrease in the magnitude of the eigenvalues holds across the scale of the alignment constraint, we expect that it is an artifact of the decrease in density of the filaments with increasing tube radius. Considering, in Figure 14, the change in magnitude of the eigenvalues for alignment constraint of 0.85, we do not see any meaningful change in magnitude with increasing tube radius as the magnitudes remain roughly constant at the largest eigenvalue measures of entanglement.

We now wish to characterize the consequences of increasing the alignment constraint for a fixed tube radius. For a tube of radius equal to 0.10, 1.00 or 5.00, in Figure 15 we see that there is a visible increase in the magnitude of the largest eigenvalue as the alignment constraint increases independent of the radius of the tube. Indeed, the actual values of the magnitude of the largest eigenvalue are quite similar, independent of the radius of the tube though a bit lower for the very largest tube.

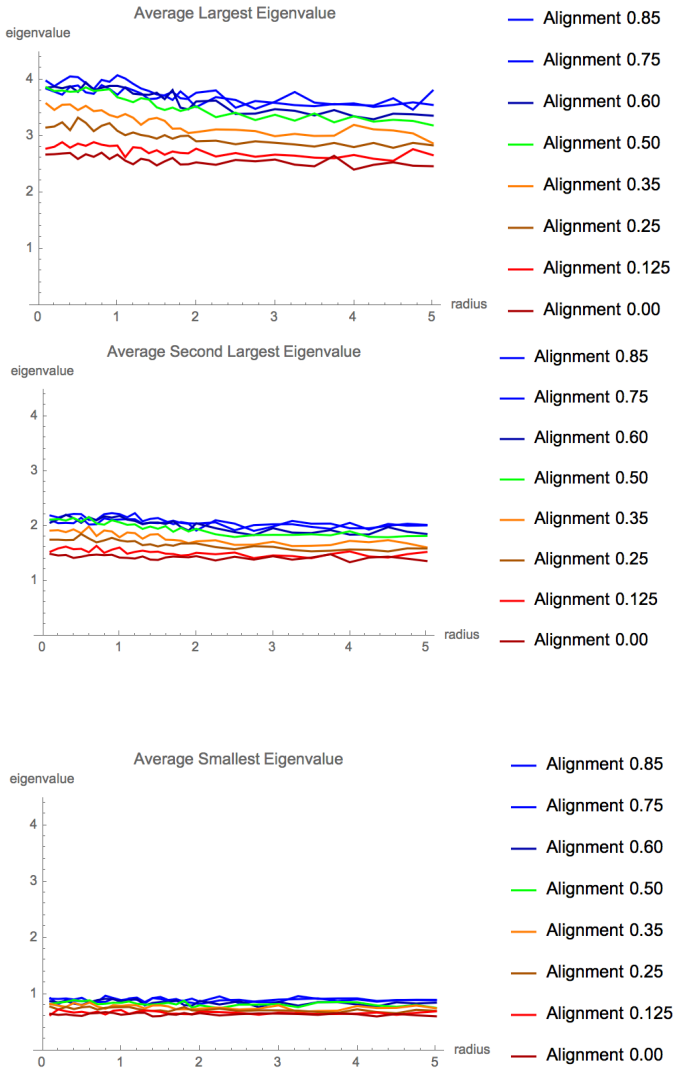

Figure 11: Effect of tube radius and alignment constraint on the mean absolute eigenvalues of a PBC system generated by three independent filaments of length 25

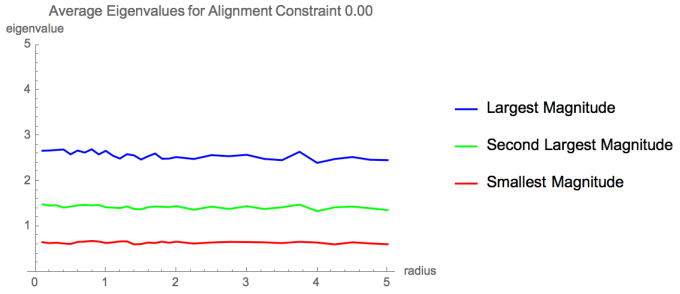

Figure 12: Effect of random alignment, fixed at 0.00, on length 25 filament; radial scale 0.10 to 5.00

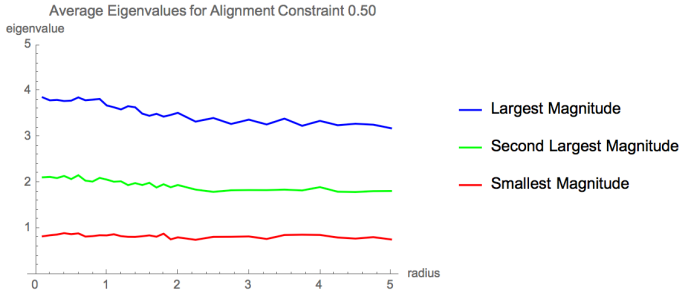

Figure 13: Effect of alignment constraint, fixed at 0.50, on length 25 filament; radial scale 0.10 to 5.00

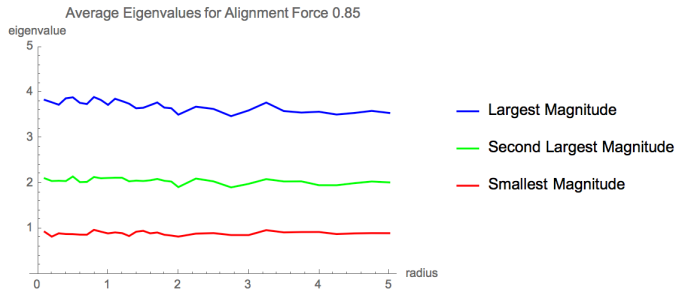

Figure 14: Effect of alignment constraint, fixed at 0.85, on length 25 filament; radial scale 0.10 to 5.00

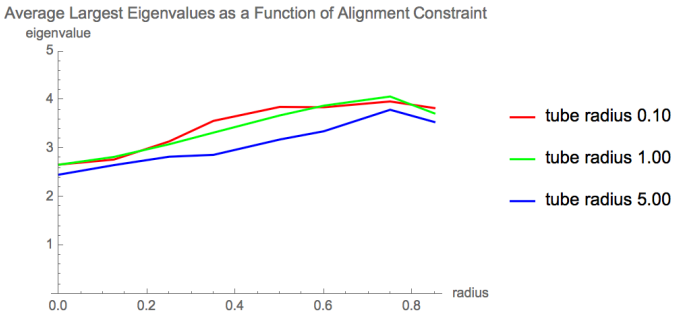

Figure 15: Effect of alignment constraint on the mean largest magnitude eigenvalue for length 25 filaments for tube radii 0.10, 1.00,and 5.00

4 Conclusions

The entanglement in polymer melts, Olympic gels, and systems of vortex flow lines is fundamentally a many body problem. Our goal is to describe its principal properties with a measure of entanglement that takes into consideration the overall conformation of the system. For this purpose we defined the linking matrix. For systems employing PBC, we then defined the periodic linking matrix using the periodic linking and self-linking measures. In the simulation of a polymer system, the size of the cell may vary. It is necessary to know how the data obtained from different cell sizes are related. By focusing on an arbitrary fixed periodic system simulated by a varying cell-size simulation box with one PBC, we proved that some of the eigenvalues of the periodic linking matrix are invariant of cell size. This information can be used to characterize such a one dimensional periodic system. This lead to results concerning the evolution of these structural measures as the size of the basic cell changes [13]. The analysis of one dimensional PBC systems was applied to Olympic systems and to tubular systems to give the results reported here [9, 12] giving new insight into the structure of these systems.

5 Acknowledgements

This research has been cofinanced by the European Union (European Social Fund — ESF) and Greek national funds through the Operational Program "Education and Lifelong Learning" of the National Strategic Reference Framework (NSRF) — Research Funding Program: THALIS.

References

[1] J Arsuaga, Y Diao, and K Hinson. The effect of angle restriction on the topological characteristics of minicircle networks. *Journal of Statistical Physics*, 146(2):434–445, 2012.

[2] J Chen, CA Rauch, JH White, PT Englund, and NR Cozarelli. The topology of kinetoplast dna network. *Cell*, 80:61 – 69, 1995.

[3] Pierre-Gilles De Gennes. *Scaling concepts in polymer physics*. Cornell University Press, 1979.

[4] Y Diao, K Hinson, and J Arsuaga. The growth of minicircle networks on regular lattices. *Journal of Physics A: Mathematical and Theoretical*, 45(3):035004, 2012.

[5] Y Diao, K Hinson, R Kaplan, M Vazquez, and J Arsuaga. The effects of density on the topological structure of the mitochondrial dna from trypanosomes. *Journal of mathematical biology*, 64(6):1087–1108, 2012.

[6] Y Diao, K Hinson, Y Sun, and J Arsuaga. The effect of volume exclusion on the formation of dna mini circle networks: implications to kinetoplast dna. *J. Phys. A: Math. Theor.*, 48:1 – 11, 2015.

[7] Gauss K F. Zur mathematischen theorie der electrodynamischen wirkungen. *Werke vol 5 Konigl. Ges. Wiss. Gottingen*, page 605, 1877.

[8] N. Hirayama, K. Tsurusaki, and T Deguchi. Linking probabilities of off-lattice self-avoiding polygons and the effects of excluded volume. *J Phys, A: Math. Theor.*, 42:105001, 2009.

[9] Spencer Igram, Kenneth C Millett, and Eleni Panagiotou. Resolving critical degrees of entanglement in olympic ring systems. *submitted to JKTR*, tbd(tbd):tbd, 2016.

[10] J. Lukes, D.L. Guilbride, J. Votypka, A. Zikova, R. Benne, and P. T. Englund. Kinetoplast dna network: Evolution of an improbable structure. *Eukaryotic Cell*, 1(4):495–502, 2002.

[11] C Micheletti, D Marenduzzo, and E Orlandini. Polymers with spatial or topological constraints: Theoretical and computational results. *Physics Reports*, 504:1 – 73, 2011.

[12] Kenneth C Millett and Eleni Panagiotou. Entanglement transitions in one-dimensional confined fluid flow. *tbd*, tbd(tbd):tbd, 2016.

[13] Kenneth C Millett and Eleni Panagiotou. The linking matrix in systems with periodic boundary conditions. *submitted SIAM*, tbd(tbd):tbd, 2016.

[14] Kenneth C Millett, Patrick Plunkett, Michael Piatek, Eric J Rawdon, and Andrzej Stasiak. Effect of knotting on polymer shapes and their enveloping ellipsoids. *The Journal of chemical physics*, 130(16):165104, 2009.

[15] E Panagiotou. The linking number in systems with periodic boundary conditions. *Journal of Computational Physics*, 2015.

[16] E Panagiotou, KC Millett, and S Lambropoulou. The linking number and the writhe of uniform random walks and polygons in confined spaces. *Journal of Physics A: Mathematical and Theoretical*, 43(4):045208, 2010.

[17] Oscar Rojo and Hector Rojo. Some results on symmetric circulant matrices and on symmetric centrosymmetric matrices. *Linear Algebra and its Applications*, 392:211–233, 2004.